MAGNETIC RESONANCE IN CHEMISTRY
Magn. Reson. Chem. 2000; **38**: 403–414

Comparative ^{13}C and ^{2}H relaxation study of microsecond dynamics of the AT tract of selectively $^{13}C/^{2}H$ double-labelled DNA duplexes

T. V. Maltseva, A. Földesi, D. Ossipov and J. Chattopadhyaya*

Department of Bioorganic Chemistry, Box 581, Biomedical Center, Uppsala University, S-751 23 Uppsala, Sweden

Received 23 September 1999; revised 20 January 2000; accepted 20 January 2000

ABSTRACT: The microsecond dynamics of the sugar moiety of **A** and **T** residues in DNA duplexes, $d^{5'}(^{1}C^{2}G^{3}\mathbf{A}^{4}\mathbf{T}^{5}\mathbf{T}^{6}\mathbf{A}^{7}\mathbf{A}^{8}\mathbf{T}^{9}C^{10}G)_2^{3'}$ (**1b**) and $d^{5'}(^{1}C^{2}C^{3}\mathbf{A}^{4}\mathbf{T}^{5}\mathbf{T}^{6}\mathbf{A}^{7}\mathbf{A}^{8}\mathbf{T}^{9}G^{10}G)_2^{3'}$ (**2b**), containing $^{13}C/^{2}H$ double-labelled 2′(*R*/*S*),5′(*R*/*S*)-$^{2}H_2$-1′,2′,3′,4′,5′-$^{13}C_5$-2′-deoxyribofuranose moieties (all labelled **A** and **T** are shown in bold), were studied using ^{13}C nuclear spin relaxation measurements. An exchange contribution was detected in the transverse relaxation rates ($R_{1\rho}$) of ^{13}C of the labelled nucleotides. The comparison of the dynamics of various nucleotide residues of duplex **1b** with those of the duplex **2b** demonstrated that the replacement of the $^{2}G{\cdot}^{9}C$ base pair in the former by a $^{2}C{\cdot}^{9}G$ base pair in the latter alters the time-scale of motions in the AT tract. Moreover, the **T** residues show different microsecond dynamic behaviour to the **A** residues in the **A**·**T** base pairs. Since ^{2}H nuclear magnetic spin relaxation ($T_{1\rho}$) measurements of the same nucleotides show no dependence on the spin lock strength, it was concluded that the main mechanism of ^{2}H $T_{1\rho}$ relaxation is quadrupolar. Although we observed a clear difference in the dynamic characteristics of the AT tract of the duplexes **1b** and **2b** [as evident from distinct differences in both spin lock dependent ^{13}C relaxation ($T_{1\rho}$) and in the amplitude of the exchange parameter amongst all deoxyadenosine nucleotide residues in both duplexes], we failed, however, to observe any difference in hydration behaviour in solution, thereby suggesting that there is no straightforward correlation in these two intrinsic dynamic properties of DNA duplex. It is noteworthy, however, that as the flexibility of the minor groove increases in both duplexes, we observe more long-lived water molecules around.

KEYWORDS: NMR; ^{13}C NMR; ^{2}H NMR; relaxation; dynamics; AT tract; DNA duplexes

INTRODUCTION

The study of dynamic motion in DNA duplex basing on the transverse relaxation rate (R_2) measurements may shed light on the correlation of its structure, stability and biological function. The main mechanism for ^{13}C relaxation in the sugar moieties of DNA involves the fluctuation of $^{13}C—^{1}H$ bond dipoles with respect to the static magnetic field (the ^{13}C CSA contribution is believed to be small for the sugar moiety[1,2]). These fluctuations result from overall tumbling motion of DNA on the nanosecond (ns) time-scale and faster external motion.[3–5] Motion on the millisecond (ms) to microsecond (μs) time-scale (chemical exchange) can also have a dramatic influence on transverse relaxation of ^{13}C. Slower than correlated rates of overall rotation can result from the relative movement of secondary structural elements of the nucleotides[6] where the degree of motion may play a role in the ligand selectivity[6] or the hydration pattern of the minor groove of the AT tract.

The dependence of transverse relaxation on static field strength[3–5,7,8] provides a direct measure of rate of exchange (K_{ex}) between two conformational states. To characterize explicit rates of exchange, the transverse relaxation rate, R_2, is monitored as a function of CPMG refocusing delay length,[3a,b,4,7] spin lock field strength[3a,c,4,5] or temperature.[6b,9a] Each of these techniques is limited to a certain range of time-scales.

It has been shown by x-ray studies that a small variation in the base-pairing sequence such as the substitution of GC basepair in C*G*ATTAAT*C*G (**1a**) with CG in C*C*ATTAAT*G*G (**2a**) causes some dramatic change in their minor groove structure and hydration pattern,[10] although they both have the same AT tract. Naturally, an important question to address here is what the dynamic difference between these two duplexesis.

The assessment of the dynamic characteristics in **1a** and **2a** can easily be done if we can compare the relaxation properties of the AT tract in the corresponding $^{13}C/^{2}H$ double-labelled derivatives **1b** and **2b**. The chemospecific incorporation of deuterium at C2′ and C5′ in the ^{13}C-labelled sugar moiety permits this because it has a remarkable benefit in the sense that it effectively helps to eliminate the cross-correlation effect of DD($^{13}C-^{1}H$) from the ^{13}C relaxation rate of the methylene protons.

* *Correspondence to*: J. Chattopadhyaya, Department of Bioorganic Chemistry, Box 581, Biomedical Center, Uppsala University, S-751 23 Uppsala, Sweden; e-mail: jyoti@bioorgchem.uu.se
Contract/grant sponsor: Swedish Board for Technical and Engineering Research (TFR).
Contract/grant sponsor: Swedish Natural Science Research Council (NFR); *Contract/grant number*: K-KU 12067-300; *Contract/grant number*: K-AA/Ku 04626-321.
Contract/grant sponsor: Wallenbergsstiftelsen.

We report here a transverse ^{13}C relaxation study ($T_{1\rho}$) of 2′(*R*/*S*),5′(*R*/*S*)-$^{2}H_{2}$-1′,2′,3′,4′, 5′-$^{13}C_{5}$-2′-deoxyadenosine and the corresponding thymidine nucleotides [bearing diastereomeric proton and deuteron in a 1 : 1 ratio at C5′, and 15% (*R*) : 85% (*S*) at C2′] in duplexes $d^{5'}(^{1}C^{2}G^{3}\mathbf{A}^{4}\mathbf{T}^{5}\mathbf{T}^{6}\mathbf{A}^{7}\mathbf{A}^{8}\mathbf{T}^{9}C^{10}G)_{2}^{3'}$ (**1b**) and $d^{5'}(^{1}C^{2}C^{3}\mathbf{A}^{4}\mathbf{T}^{5}\mathbf{T}^{6}\mathbf{A}^{7}\mathbf{A}^{8}\mathbf{T}^{9}G^{10}G)_{2}^{3'}$ (**2b**) in aqueous solution. The site-specific incorporation of $^{13}C/^{2}H$-double-labelled dA and T blocks in **1b** and **2b** was achieved by the solid-phase synthesis protocol. We attempted to explore whether the dynamics in the microsecond range drive any specific water–DNA interaction by inducing any large conformational transitions. This was performed by comparing our NMR-based dynamic and hydration data for duplexes **1b** and **2b** in aqueous solution with the hydration data reported using the x-ray studies of the corresponding unlabelled duplexes, **1a** and **2a**.

EXPERIMENTAL

Synthesis of double-labelled ^{13}C–^{2}H nucleosides and DNA

The syntheses of double-labelled $^{13}C/^{2}H$ nucleosides were performed using our published procedure.[11] The double-labelled 10 mers **1b** and **2b** were prepared by the solid-phase phosphoramidite method[12] on a Pharmacia LKB Gene Assembler Special synthesizer. Finally, the purified sample (237 O.D. units, 13% yield) was loaded on a Dowex 50-WX (Na^{+}) column, then lyophilized together with the appropriate buffer used for NMR spectroscopy from D_2O (99.9% D).

NMR experiments

The NMR experiments were carried out on Bruker DRX spectrometers at a magnetic field strength of 14.1 T, operating at 600.13 MHz for ^{1}H, 150.92 MHz for ^{13}C and 92.12 MHz for ^{2}H, and at a magnetic field strength of 11.7 T operating at 500.03 MHz for ^{1}H, 125.74 MHz for ^{13}C and 76.76 MHz for ^{2}H. Both spectrometers were equipped with a Bruker digital lock and with a switching ^{2}H lock–^{2}H pulse device.

The 600.13 MHz spectrometer was equipped with an inverse detection quadro-resonance probehead with triple axis gradients for ^{1}H, ^{13}C, ^{31}P and ^{15}N (QXI). Hard ^{1}H pulses on this probehead were applied with 29 kHz. ^{13}C hard and selective 2.5 ms e_burp_1 pulses were applied with a 19.2 kHz and 1250 Hz field peak strengths, respectively. ^{13}C decoupling was performed using GARP[13a] with a 3.84 kHz field strength. For the 90° and 180° ^{2}H pulses the probe power after the switching block was 6.4 W, which corresponds to 2.08 kHz applied field. ^{2}H decoupling utilised a WALTZ16[13b] sequence using a 588 Hz field.

The 500.03 MHz spectrometer was equipped with a triple-resonance selective probehead for ^{13}C and ^{2}H (TXO). ^{1}H and ^{13}C pulses were applied with 24 and 40 kHz field, respectively. This strength of ^{13}C pulses allowed us to excite the region between $^{13}C(5')$ and $^{13}C(2')$ resonances and neglected the offset effect on measurement of $T_{1\rho}$ relaxation of ^{13}C as we have shown earlier in our relaxation study on deuterated nucleosides.[2] ^{13}C decoupling was performed using GARP with a 4.17 kHz field strength. For the 90° and 180° ^{2}H pulses, the probehead power after the switching block was 43.0 W, which corresponds to 11.4 kHz applied field. ^{2}H decoupling utilized a WALTZ16 sequence using a 1.3 kHz field (0.6 W).

All experiments were carried out at 25 °C. This temperature is more then 20 °C below the melting temperature of these duplexes (47–50 °C) at the NMR concentration of the samples and the buffer composition.

Determination of $T_{1\rho}$ relaxation time of ^{13}C by 2D experiment. Figure 1(A) shows the pulse sequence used to determine ^{13}C $T_{1\rho}$ relaxation. During ^{13}C chemical shift evolution in the t_1 period the constant time period to eliminate ^{13}C–^{13}C couplings was implied[1] and the WALTZ16 modulation on deuterium was used to decouple ^{13}C from deuterium. The train of ^{1}H 125° pulses was applied every 5 ms before the first soft ^{13}C pulse in the same way as originally proposed.[14b] Magnetization originating from ^{13}C nucleus was transferred to the directly bound protons for detection using an INEPT-type module.[1,14b]

The experiments were carried out at a magnetic field strength of 14.1 T.

The data sets were recorded as 2K × 96 real matrix with 64 scans for ^{13}C relaxation measurement for each t_1 value and a spectral width of 10 ppm in F_2 and 20 ppm in F_1 with the carrier for ^{1}H, ^{13}C, ^{2}H at 4.8, 82.84 [for $^{13}C(1')$, $^{13}C(4')$] or 37.44 [for $^{13}C(2')$] and 3.25 ppm, respectively.

The strength of the spin locking field, ω_1, was determined by finding the pulse length, $t_{360°}$, required to produce a signal null following a 360° rotation of the observed line about ω_{SL} according to $\omega_1 = 2\pi/t_{360°}$. Ten data sets with different ^{13}C spin lock field (SL_y) was used in the $T_{1\rho}$ measurements, $\omega_1/2\pi$ = 4166, 3333, 2778, 2173, 2000, 1667, 1351, 961, 806 and 760 Hz. At each ^{13}C spin lock field (SL_y), the total duration of the spin lock set typically by looping of two 2 ms SL pulses, interrupted by a 180° ^{1}H pulse to minimize the effects of cross-relaxation and from intramolecular dipole and CSA cross-correlation, n times was varied 4, 8, 12, 15, 20, 24, 32, 40, 48, 60 and 80 ms to obtain a series of 11 experiments of $T_{1\rho}$ measurements.

To ensure that the magnetization of the observed resonance was aligned in the rotating frame along a transverse effective field for all values of ω_1, the frequency of the r.f. carrier, ω, was set at the middle of ^{13}C interval of interest with the largest deviation (offset, $\Delta\omega_i$, between the carrier and the resonance frequency of the ith species) was 200 Hz. The off-resonance contribution was evaluated according to[7,15]

$$R_{1\rho}(^{13}C) = R_1(^{13}C)\cos^2(\phi) + R_2(^{13}C)\sin^2(\phi)$$
$$\sim R_2(^{13}C)\sin^2(\phi)$$

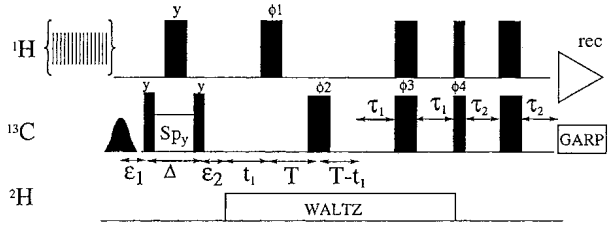

Figure 1. Pulse sequence used to measure the transverse relaxation time, $T_{1\rho}$, of ^{13}C. All narrow (wide) pulses are applied with flip angles of 90° (or 180°) and are along the *x*-axis, unless indicated otherwise. The carriers of ^{1}H, ^{2}H are positioned at 4.8 and 3.25 ppm, respectively, while the ^{13}C carrier is set at 82.84 [for $^{13}C(1')$, $^{13}C(4')$] or 37.44 [for $^{13}C(2')$]. All proton pulses are adjusted in every experiment to maximum strength. The ^{13}C hard pulses use a 19.2 kHz field, while decoupling during acquisition is achieved with GARP sequence[13a] with a 3.84 kHz field strength. The ^{13}C shaped pulse is applied as e_burp_1[39] type profile, of duration 2.5 ms (1250 Hz peak r.f.). ^{2}H decoupling utilised a WALTZ16[13b] sequence using a 588 Hz field strength. Development of the NOE via non-selective saturation of ^{1}H resonances is accomplished with 135° ^{1}H pulses separated by 5 ms shown in pre-scan delay during 1.5 s in parentheses. Two 2 ms SL pulses, interrupted by a 180° ^{1}H pulse to minimize the effects of cross-relaxation and from intramolecular dipole and CSA cross-correlation. The delays used are $\tau_1 = 1.33$ ms in the way proposed,[14b,40] $\tau_2 = 1/8J(C,H) = 0.9$ ms in the way a proposed[14b] to minimize the effects of differential ^{1}H relaxation. The *T* delay in a constant time period was set at 26.6 ms. The delays ε_1 and ε_2 are set according to the literature procedure[41] to eliminate the offset dependence: $\varepsilon_1 = 1/(2\pi\nu_1) - (4/\pi)t_{90°}$, where the strength of the spin lock field (ν_1) equals $\omega_1/2\pi$, and $t_{90°} = 90°$ pulse length of the ^{13}C and $\varepsilon_2 = 1/(2\pi\nu_1)$. The phase cycling employed was $\phi_1 = 4(x), 4(-x)$; $\phi_2 = 16(y), 16(-x)$; $\phi_3 = x, y, -x, -y$; $\phi_4 = 8(y), 8(-y)$; rec $= 4(x, -x), 8(-x, x), 4(x, -x)$. Quadrature detection in F_1 was achieved by TPPI of ϕ_4.

where $\cos(\phi) = \Delta\omega_i/\sqrt{(\Delta\omega_i^2 + \omega_1^2)}$ and $\sin(\phi) = \omega_1/\sqrt{(\Delta\omega_i^2 + \omega_1^2)}$. Under the conditions of the experiments, the $\sin^2(\phi)$ values ranged from 0.93 to 1, which is below the experimental error.

These experiments were performed in random order, with respect to both refocusing delay and mixing time, in order to minimize systematic errors. In all cases the recycle delay was 2.0 s. The acquisition time for each experiment was 6 h for a total of 66 h per data set.

To evaluate the influence of offset on quantitative measurement of transverse relaxation rate for duplex **1b**, two data sets of ^{13}C $T_{1\rho}$ from spin lock field were collected at a carrier frequency of 12 675 Hz (on-resonance with ^{3}**A**, ^{7}**A**, ^{5}**T**, ^{4}**T**, ^{8}**T**) and 12 398 Hz (on-resonance with ^{6}**A**), leading to an offset of 277 Hz. Within the experimental error no difference was observed and hence no correction of the effective spin lock field[16] was applied. For duplex **2b** the carrier frequency was at 12 502 Hz.

Determination of T_1 relaxation time of ^{13}C by 2D experiment. The ^{13}C T_1 values were measured using the pulse sequence proposed earlier by King *et al.*[1] with the only difference that during ^{13}C chemical shift evolution in the t_1 period the constant time period to eliminate ^{13}C–^{13}C coupling was applied and WALTZ16 modulation on deuterium was used to decouple ^{13}C from deuterium. All experimental conditions were identical with those used in $T_{1\rho}$ relaxation measurements of ^{13}C by 2D experiment and carried out at a magnetic field strength of 14.1 T. The total recovery time was typically set by looping of two 5 ms delays, interrupted by ^{1}H 125° pulses to minimize the effects of cross-relaxation and from intramolecular dipole and CSA cross-correlation, *n* times was varied, 10, 20, 40, 60, 100, 150, 200, 300, 400, 500, 600, 700 and 1000 ms, to obtain a series of 13 experiments, which were used for the T_1 measurements.

Determination of $T_{1\rho}$ relaxation time of ^{2}H by 2D experiment. The ^{2}H $T_{1\rho}$ values were measured using the pulse sequence proposed earlier[12] at a magnetic field strength of 11.7 T. Carriers were positioned at 4.8 ppm for ^{1}H and ^{2}H in all experiments; 65 ppm in the $^{13}C(5')$ area, 40 ppm in the $^{13}C(2')$ area. The spectra were recorded with acquisition times of 15.5 and 204.8 ms in (t_1, t_2) as 78×2048 or 12.7 and 204.8 ms in (t_1, t_2) as 256×2048 complex matrices depending on the sweep width used for carbon, 20 or 80 ppm.

Ten data sets with different ^{2}H spin lock field (SL_y) were used in the $T_{1\rho}$ measurements in the range 11.4–1.25 kHz. At each ^{2}H spin lock field (SL_y), the $T_{1\rho}$ measurements were used in a series of 10 experiments with relaxation times of 0.02, 0.2, 0.4, 0.6, 0.8, 1.0, 1.5, 2.0, 2.5 and 3 ms. In all cases the recycle delay was 1 s. The acquisition time for each experiment was 6 h for a total of 66 h per data set.

To avoid the spinning artefacts, all spectra were measured on non-spinning samples.

Data evaluation in 2D experiments. The spectra were processed and analysed on a Silicon Graphics workstation using XWINNMR (v. 2.1) and AURELIA programs (Bruker). For the evaluation of the $T_{1\rho}$ of ^{2}H and ^{13}C and T_1 of ^{13}C the volumes of cross peaks in a series of 2D spectra were fitted to a single exponential, depending on the relaxation delay, using the equation

$$V(\Delta) = V(0)\exp(-\Delta/T_1), \qquad (1)$$

where $T_{1\rho}$ is the relaxation time of ^{2}H and ^{13}C or T_1 of ^{13}C, $V(\Delta)$ and $V(0)$ are the volumes of cross peaks at time Δ (defined in Fig. 1 as delay Δ) and zero time, respectively.

The fit was performed using a least-squares minimization procedure using the program PROFIT (v. 4.2). The monoexponential character of the decay was tested using Monte Carlo procedures as established.[14]

Conformation exchange on the microsecond timescale. The techniques for the identification and evaluation of the exchange rate (K_{ex}) of the conformational exchange in a two-state model (A and B) by varying the amplitude of the spin lock field applied to the ^{13}C magnetization in the rotating frame has been considered numerically.[3,4,7]

$K_{ex}(1/\tau_{ex})$ can be derived by fitting the observable transverse relaxation rate ($R_{1\rho} = 1/T_{1\rho}$), measured in the CT-$T_{1\rho}$ experiment (Fig. 1), to the equation

$$\frac{1}{T_{1\rho}} = p_A p_B \Delta\Omega^2 \frac{\tau_{ex}}{1 + (\omega_1 \tau_{ex})^2} + \frac{1}{T_{1\rho}^{\infty}} \qquad (2)$$

where p_A and p_B are the arbitrary populations, $\Delta\Omega = \Omega_A - \Omega_B$, with Ω_A and Ω_B being the chemical shifts of the spins in the states A and B (in rad s^{-1}), relative to the ^{13}C carrier frequency. ω_1 is the applied r.f. spin lock field, $1/T_{1\rho}^{\infty}$ is the relaxation time for an infinitely large spin lock power, $K_{ex} = k_{A-B} + k_{B-A} = 1/\tau_{ex}$, where k_{A-B} and k_{B-A} are the forward and reverse reaction constants, and K_{ex} is the rate constant of exchange. Equation (2) is valid only if $\Delta\Omega\tau_{ex} \ll 1$.[3d,7]

Hydration experiments. Phase-sensitive NOESY experiments with water suppression were carried out at a magnetic field strength of 11.7 T by the use of two short spin lock pulses, $SL_{\varphi 4}$ and $SL_{\varphi 5}$, as described,[17,18] using the following parameters: mixing times (τ_m) were varied between 0.06 and 0.160 s to observe the spatial contact of the non-exchangeable protons with water; 4 K complex data points in t_2, 512 complex data points in t_1, the relaxation delay between pulse sequences was 2.0 s, $SL_{\varphi 4}$ and $SL_{\varphi 5}$ were equal to 0.5 and 3 ms, respectively, the delay between spin lock pulses τ was equal to 167 μs, the carrier was set at the water frequency and 32 scans/FID were used for quadrature detection in the F_1 dimension with time-proportional phase incrementation (TPPI). 2D data sets for ROESY spectra with water suppression were achieved with one short spin lock pulse, $SL_{\varphi 3}$.[17,18] During the mixing a time sequence of $n(\pi/6)$ pulses with length 3.4 μs separated by delay Δ (34.5 μs) provides a similar effect as spin lock $SL_{\varphi 4}$ of the NOESY experiment, so that the spectra were recorded with spin lock duration between 0.03 and 0.08 s using a 6.25 kHz r.f. field for all pulses and a recycle delay of 2 s. Typically 4K data points were collected for each t_1 512 values during experiments. A 3 ms saturation pulse was applied after data acquisition. The spectral excitation profile in these experiments was proportional to $\sin(\Omega\tau)$, where Ω is the angular frequency relative to the carrier and $\tau = 167$ μs. The non-uniform spectral excitations in the F_2 dimension were corrected by multiplying by $1/\sin(\Omega\tau)$.

The sign of the cross peak was compared with the diagonal peaks, which were assumed to be positive.[17,18]

The assignment of all protons of duplexes **1b** and **2b** was done in a conventional manner, using NOESY and DQF-COSY experiments. They will be published elsewhere together with our structural analysis.

UV measurements. UV melting profiles were obtained by scanning the absorbance at 260 nm versus time at a heating rate of 1 °C min^{-1} with a temperature gradient of 15–65 °C (50 min). The T_m values were calculated from the maxima of the first derivatives of the melting curves with an accuracy of 0.5 °C. The T_m values used for the thermodynamic calculations were taken from the average of five melting experiments for the each concentration. All measurements were carried out in 0.1 M Na_2HPO_4–NaH_2PO_4, 1 M NaCl buffer at pH 7.0. Before each melting experiment, denaturation and renaturation of the samples were carried out by heating solutions to 65 °C for 3 min followed by slow cooling to room temperature and storage in 15 °C for 30 min.

Melting points for six different oligonucleotide concentrations (10, 12, 14, 16, 18 and 20 μM total single strand concentration) were measured for the thermodynamic calculations. The resulting T_m values were fitted to a van't Hoff plot of T_m^{-1} versus $\ln(C_T)$. The thermodynamics were calculated using the following equations:

$$1/T_m = (R/\Delta H^\circ)\ln C_T + \Delta S^\circ/\Delta H^\circ$$

$$R/\Delta H^\circ = \text{slope}$$

$$\Delta S^\circ/\Delta H^\circ = \text{intercept}$$

$$\Delta G^\circ(298\,K) = \Delta H^\circ - T\Delta S^\circ$$

where C_T is the total single strand concentration.

RESULTS

Measurement of $T_{1\rho}$ of ^2H

The $T_{1\rho}$ of $^2H(2'')$ was measured for the sugar moieties of all six **A** and **T** residues in duplex **1b** using the pulse sequence published earlier.[12] In the range 11.4–1.25 kHz spin lock strength, there was no variation observed for $T_{1\rho}$ of $^2H(2'')$ with a 10% error. This is in agreement with the theoretical expectation [Eqn (2)] (see also Ref. 3a, Fig. 6): $1/T_{1\rho}^{\infty}$ is very large ($\sim 500\ s^{-1}$) compared with the same value for ^{13}C ($11.76\ s^{-1}$) because the main mechanism of $T_{1\rho}$ relaxation for ^2H is quadrupolar in nature. The average values of $T_{1\rho}$ of $^2H(2'')$ for nine experiments at different spin lock power experiments with their standard deviations were as follows: for **A** residues, 1.45 ± 0.26 ms (^{6}**A**), 1.51 ± 0.16 ms (^{3}**A**), 1.54 ± 0.17 ms (^{7}**A**), and for **T** residues, 1.68 ± 0.19 ms (^{4}**T**), 1.94 ± 0.21 ms (^{5}**T**), 1.95 ± 0.20 ms (^{8}**T**). As has been mentioned earlier,[12] the $T_{1\rho}$ and T_1 of $^2H(2'')$ for the **A** residues are shorter than for the **T** residues, which presumably is due to the difference in order parameter. Since the present study shows that the $T_{1\rho}$ of $^2H(2'')$ is not sensitive to conformational exchange on the microsecond scale in contrast to the $T_{1\rho}$ of $^{13}C(2')$, the ratio of longitudinal, $T_1[^2H(2'')]$, to transverse relaxation time, $T_{1\rho}[^2H(2'')]$, does not depend on an order parameter, and it could be used to elucidate the overall correlation time of the molecule. These ratios were as follows for duplex **1b**: 4.19 ± 0.47 (^{3}**A**), 4.29 ± 0.79 (^{6}**A**), 4.59 ± 0.52 (^{7}**A**), 4.14 ± 0.47 (^{4}**T**), 4.41 ± 0.48 (^{5}**T**), 4.73 ± 0.50 (^{8}**T**). These ratios gave an overall correlation time of $\sim 3.5 \pm 0.5$ ns.

Measurement of $T_{1\rho}$ of $^{13}C(1')$

Transverse relaxation rates ($R_{1\rho}$) of ^{13}C were measured in the sugar moieties (at C1′, C2′ and C4′) of six **A** and

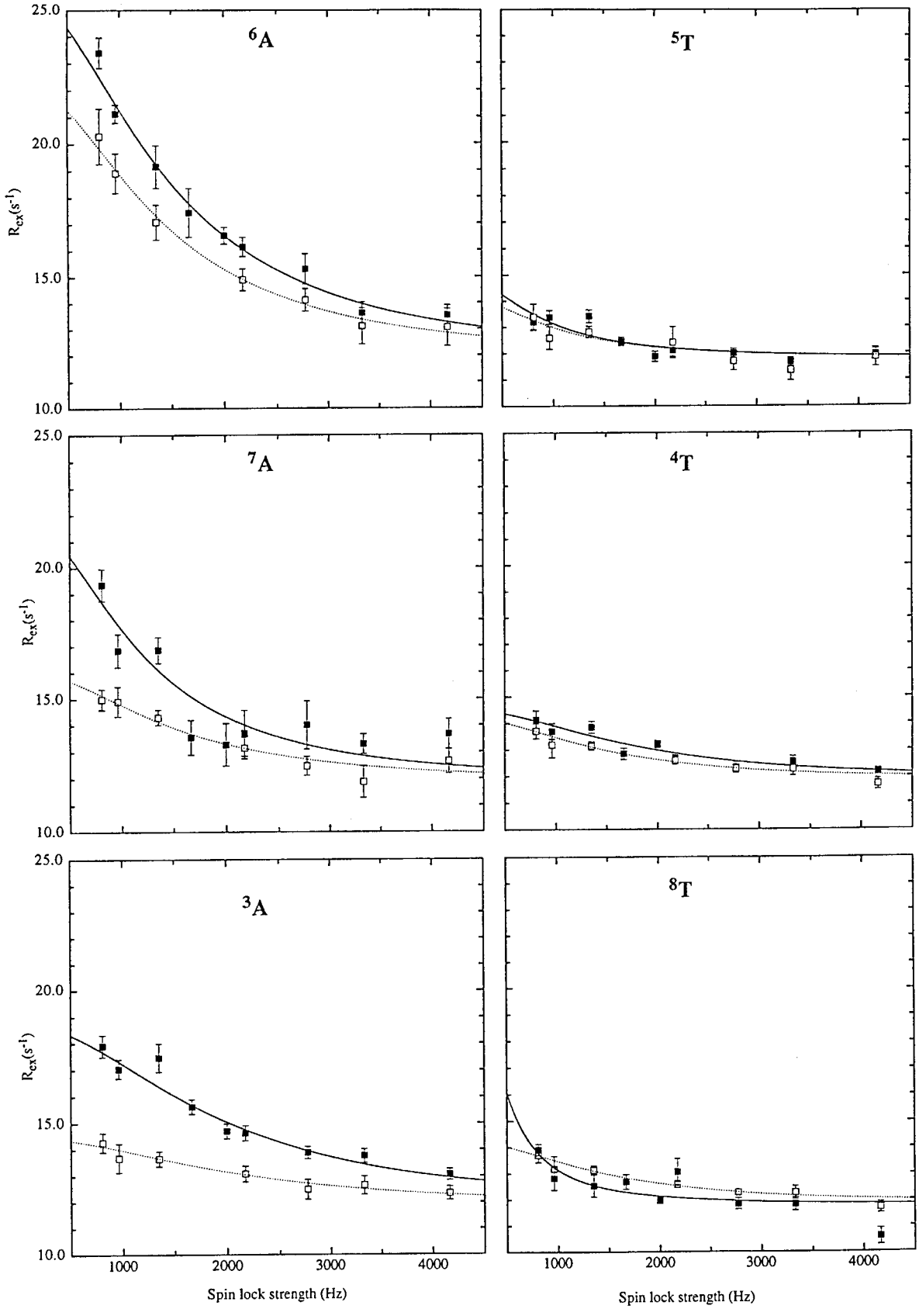

Figure 2. Transverse relaxation rates, $R_{1\rho}$, of $^{13}C(1')$ plotted against effective field strength of spin lock, $\omega_1/2\pi$, for six residues (panels are marked with names of residues) in duplexes $d^{5'}(^1C^2G^3\mathbf{A}^4\mathbf{T}^5\mathbf{T}^6\mathbf{A}^7\mathbf{A}^8\mathbf{T}^9C^{10}G)_2^{3'}$ (**1b**) (□) and $d^{5'}(^1C^2C^3\mathbf{A}^4\mathbf{T}^5\mathbf{T}^6\mathbf{A}^7\mathbf{A}^8\mathbf{T}^9G^{10}G)_2^{3'}$ (**2b**) (■) at 25 °C. Error bars represent the standard deviation of $R_{1\rho}$. The dashed and solid curves for the duplexes **1b** and **2b**, respectively, are the best least-squares fits of Eqn (2) with τ_{ex} and $\Delta\Omega$ as free variables. The best fits were obtained with $1/T_{1\rho}^{\infty} = 11.76\,s^{-1}$.

T residues in the isomeric DNA decamers $d^{5'}(^1C^2G^3\mathbf{A}^4\mathbf{T}^5\mathbf{T}^6\mathbf{A}^7\mathbf{A}^8\mathbf{T}^9C^{10}G)_2^{3'}$ (**1b**) and $d^{5'}(^1C^2C^3\mathbf{A}^4\mathbf{T}^5\mathbf{T}^6\mathbf{A}^7\mathbf{A}^8\mathbf{T}^9G^{10}G)_2^{3'}$ (**2b**) using the pulse sequence presented in Fig. 1.

By plotting $R_{1\rho}$ of $^{13}C(1')$ against ω_1 [Eqn (2)], two categories of residues were identified (Fig. 2): (1) In the first set where all **T** residues could be included, the $R_{1\rho}$ of ^{13}C shows a very modest variation with ω_1. Moreover, at higher strength of spin lock, the $R_{1\rho}$ of ^{13}C are approximately the same for all residues ($11.76\,s^{-1}$, see Table 1) in both duplexes **1b** and **2b**. It is noteworthy that at all strengths of spin locks the values of the rate constants for the corresponding residues of the two different duplexes **1b** and **2b** are very similar within the experimental error. There are two possible explanations that $R_{1\rho}$ does not vary with ω_1: (i) that on the microsecond time-scale the **T** residues of both duplexes have no exchange motions (at least with large amplitudes); (ii) the second possibility is that the chemical exchange takes place on a very fast time-scale[7], which was ruled out on the grounds that the significant increase in $R_{1\rho}$ of $^{13}C(1')$ values of **T** residues compared with **A** residues have not been observed (Table 1). (2) In the second set with all **A** residues (^{6}**A**, ^{7}**A**, ^{3}**A**) (Fig. 2), it was found that $R_{1\rho}$ of $^{13}C(1')$ in both duplexes **1b** and **2b** are notably dependent on the spin lock strength. This means that the chemical exchange occurs on the microsecond time-scale. Nevertheless, in contrast to the **T** residues, the **A** residues show a clear discrepancy both between each other within the same duplex and between the corresponding residues for the different duplexes **1b** and **2b**.

To obtain quantitative data about the amplitude, $D = P_A P_B \Delta\Omega^2$, and chemical exchange time, τ_{ex}, the experimental data of $R_{1\rho}$ of $^{13}C(1')$ have been fitted to Eqn (2). As has been mentioned above, the term $1/T_{1\rho}^{\infty}$ in Eqn (2) mainly represents the dipole–dipole contribution for the transverse relaxation rate, and could be identified at an infinitely large spin lock power. At the largest spin lock strength used in this study (4166 Hz), the $R_{1\rho}$ of $^{13}C(1')$ were slightly different between **A** and **T** residues (Table 1). Nevertheless, the longitudinal relaxation time (T_1) of $^{13}C(1')$ of these residues (Table 1) varies around 483 ± 20 ms, which has a 5% experimental error. These data lead us to assume that the $R_{1\rho}$ of $^{13}C(1')$ difference between **A** and **T** residues is due to the contribution of the exchange term (K_{ex}). In the simulation procedure the same value of $1/T_{1\rho}^{\infty}$ was used for all residues and the best fit was obtained with $1/T_{1\rho}^{\infty} = 11.76\,s^{-1}$. The experimental data and the best fit curves are presented in Fig. 2 and data for the amplitudes and τ_{ex} are listed in Table 2. The main results could be summarized as follows: (i) the amplitudes of conformational exchange of **A** residues for both duplexes **1b** and **2b** are increased from the 5′-end of the ^{3}**A** residue to the central ^{6}**A** residue, reaching exchange with the most significant amplitudes (Table 2); (ii) the amplitudes of exchange of **A** residues for duplex **2b** are larger than in duplex **1b**; (iii) the lowest amplitudes of exchange are in the **T** residues.

The ratio of transverse, $T_{1\rho}^{\infty}[^{13}C(1')]$, to longitudinal, $T_1[^{13}C(1')]$, relaxation times was used to elucidate the overall correlation time of the molecule. This ratio, 1.75, is an average for all residues and gives an overall correlation time of $\sim 3.5 \pm 0.5$ ns, which is the same as that determined above through deuterium relaxation.

Measurement of $T_{1\rho}$ of $^{13}C(2')$

Figure 3 shows the plot of $R_{1\rho}$ of $^{13}C(2')$ against ω_1. Compared with $^{13}C(1')$, the values of $1/T_{1\rho}^{\infty}$ for $^{13}C(2')$ are different for different nucleotides. Three categories of nucleotide residues were identified. The first group includes **A** residues. They have comparable longitudinal, T_1, and transverse, $T_{1\rho}$, (at 4166 Hz spin lock power) relaxation rates for $^{13}C(1')$ and $^{13}C(2')$ (Table 1). The value of $1/T_{1\rho}^{\infty} = 11.76\,s^{-1}$ was used for simulation of the curves of these residues. The second group includes ^{8}**T** and ^{5}**T**

Table 1. Comparison of the longitudinal (T_1) and transverse ($T_{1\rho}$) relaxation times (ms) of ^{13}C nuclei for different residues of the isomeric DNA decamers $d^{5'}(^1C^2G^3\mathbf{A}^4\mathbf{T}^5\mathbf{T}^6\mathbf{A}^7\mathbf{A}^8\mathbf{T}^9C^{10}G)_2^{3'}$ (**1b**) and $d^{5'}(^1C^2C^3\mathbf{A}^4\mathbf{T}^5\mathbf{T}^6\mathbf{A}^7\mathbf{A}^8\mathbf{T}^9G^{10}G)_2^{3'}$ (**2b**) at 298 K (600 MHz)

Type of residue	Duplex	$^{13}C(C1')^a$		$^{13}C(C2')^a$	
		T_1	$T_{1\rho}^b$	T_1	$T_{1\rho}^b$
^{3}A	**1b**	471.4 ± 8.8	81.0 ± 1.7	445.2 ± 12.4	82.6 ± 3.4
	2b	464.2 ± 5.7	72.6 ± 3.0	430.2 ± 10.7	72.0 ± 5.0
^{4}T	**1b**	495.4 ± 4.1	85.5 ± 1.5	450.3 ± 16.8	86.1 ± 6.3
	2b	511.6 ± 6.8	80.0 ± 2.0	498.3 ± 10.3	91.0 ± 2.0
^{5}T	**1b**	498.7 ± 10.3	84.4 ± 2.6	486.3 ± 14.0	104.5 ± 2.9
	2b	487.9 ± 5.6	84.0 ± 2.0	507.9 ± 9.5	106.0 ± 3.0
^{6}A	**1b**	484.6 ± 12.7	76.6 ± 4.2	406.6 ± 30	91.9 ± 8.0
	2b	482.8 ± 13.2	73.0 ± 5.0	482.4 ± 15.3	75.0 ± 4.0
^{7}A	**1b**	481.6 ± 9.1	79.0 ± 2.9	452.6 ± 24.9	89.9 ± 5.1
	2b	462.7 ± 12.0	73.0 ± 2.0	448.1 ± 20.1	83.0 ± 4.0
^{8}T	**1b**	495.4 ± 4.1	85.5 ± 1.5	496.74 ± 28.9	108.8 ± 5.9
	2b	493.44 ± 8.2	84.0 ± 5.0	511.9 ± 9.3	115.0 ± 5.0

[a] The error is the standard deviation obtained in fitting experimental data to Eqn (1).
[b] At spin lock power 4166 Hz.

Table 2. Comparison of the amplitude of exchange ($D = p_A p_B \Delta\Omega^2$) and time of exchange ($\tau_{ex} = 1/K_{ex}$) of $^{13}C(1')$ and $^{3}C(2')$ nuclei for different residues of the isomeric DNA decamers: $d^{5'}(^{1}C^{2}G^{3}\mathbf{A}^{4}\mathbf{T}^{5}\mathbf{T}^{6}\mathbf{A}^{7}\mathbf{A}^{8}\mathbf{T}^{9}C^{10}G)_2^{3'}$ **(1b)** and $d^{5'}(^{1}C^{2}C^{3}\mathbf{A}^{4}\mathbf{T}^{5}\mathbf{T}^{6}\mathbf{A}^{7}\mathbf{A}^{8}\mathbf{T}^{9}G^{10}G)_2^{3'}$ **(2b)**

Type of residue and nuclei	Duplex	$D(\times 10^4\ \mathrm{rad^2\ s^{-2}})$	τ_{ex} (μs)	Type of residue	Duplex	$D(\times 10^4\ \mathrm{rad^2\ s^{-2}})$	τ_{ex} (μs)
$^{3}A(1')$	**1b**	3.54 ± 0.42	77 ± 17	$^{8}T(1')$	**1b**	2.27 ± 0.17	110 ± 20
	2b	8.26 ± 0.27	85 ± 6		**2b**	3.00 ± 1.50	500 ± 60
$^{7}A(1')$	**1b**	4.06 ± 0.36	108 ± 23	$^{4}T(1')$	**1b**	2.27 ± 0.17	110 ± 20
	2b	7.46 ± 0.39	139 ± 23		**2b**	3.08 ± 0.17	91 ± 13
$^{6}A(1')$	**1b**	9.44 ± 0.53	113 ± 16	$^{5}T(1')$	**1b**	1.53 ± 0.31	169 ± 116
	2b	12.72 ± 0.33	111 ± 7		**2b**	1.76 ± 0.22	194 ± 62
$^{3}A(2')$	**1b**	3.26 ± 0.71	67 ± 31	$^{8}T(2)$	**1b**	2.20 ± 0.44	148 ± 79
	2b	6.06 ± 0.44	61 ± 8		**2b**	31.6 ± 0.64	304 ± 98
$^{7}A(2')$	**1b**	5.95 ± 0.82	180 ± 51	$^{4}T(2')$	**1b**	4.35 ± 1.14	66 ± 28
	2b	7.99 ± 1.80	310 ± 120		**2b**	2.33 ± 0.60	281 ± 141
$^{6}A(2')$	**1b**	10.83 ± 0.97	133 ± 31	$^{5}T(2')$	**1b**	3.99 ± 0.39	118 ± 26
	2b	12.64 ± 0.54	81 ± 7		**2b**	4.13 ± 0.25	93 ± 11

residues. The value of $1/T_{1\rho}^{\infty} = 8.7\ \mathrm{s^{-1}}$, which corresponds to 115 ms, was used. It is noteworthy that it is impossible to obtain an appropriate simulation of experimental curves for $^{8}\mathbf{T}$ and $^{5}\mathbf{T}$ residues with $1/T_{1\rho}^{\infty} = 11.76\ \mathrm{s^{-1}}$, and the same is true for the reverse case.

Moreover, the longitudinal relaxation times, $T_1^{13}C(2')$, of the **A** residues are also shorter than for $^{8}\mathbf{T}$ and $^{5}\mathbf{T}$ residues, on average 445 and 505 ms, respectively. The same tendency has been mentioned above for the $T_{1\rho}$ and T_1 of $^{2}H(2'')$: they are shorter for **A** residues than for **T** residues. The third group includes the $^{4}\mathbf{T}$ residue which has $1/T_{1\rho}^{\infty} = 10.5\ \mathrm{s^{-1}}$. Indeed, $T_{1\rho}$ of $^{2}H(2'')$ for $^{4}\mathbf{T}$ residue is shorter than for $^{8}\mathbf{T}$ and $^{5}\mathbf{T}$ residues but longer than for the **A** residues. The same trend is also observed for $T_1^{13}C(2')$ relaxation data.

The amplitudes and τ_{ex} are obtained by fitting the experimental curves of Fig. 3 to Eqn (2) (Table 2).

The fact that $T_1^{13}C(1')$ and $T_1^{13}C(2')$ and also $T_{1\rho}^{13}C(1')$ and $T_{1\rho}^{13}C(2')$ are different for some residues suggests a difference in their order parameters and possibly in the correlation time of their external motions. Despite this difference, the microsecond dynamic characteristics for $^{13}C(1')$ and $^{13}C(2')$ are reasonably correlated (Table 2).

Indeed, the amplitudes of conformation exchange of $^{13}C(2')$ presented as the parameter $D = P_A P_B \Delta\Omega^2$ in Table 2, increase from the $^{3}\mathbf{A}$ residue to central $^{6}\mathbf{A}$ in the same way as for $^{13}C(1')$.

The errors of simulation of experimental curves for T residues are much higher owing to the modest dependence of the $R_{1\rho}^{13}C(2')$ and $R_{1\rho}^{13}C(1')$ rates, but in general they show conformation exchange with exchange time $(1-3) \times 10^{-4}$ s with D variation $(1-4) \times 10^4\ \mathrm{rad^2\ s^{-2}}$.

This shows that the contribution of conformational dynamics of the sugar moiety itself on the microsecond time-scale could not be distinguished in the comparative study of $^{13}C(1')$ and $^{13}C(2')$ within the range of the experimental error. The possible reason is that the two-state pseudo-rotational equilibrium between the North and South conformations[19] takes place on a faster dynamic time-scale ($10^{-9}-10^{-12}$ s).

Hydration pattern in the DNA decamers: $d^{5'}(^{1}C^{2}G^{3}A^{4}T^{5}T^{6}A^{8}T^{9}C^{10}G)_2^{3'}$ (1b) and $d^{5'}(^{1}C^{2}C^{3}A^{4}T^{5}T^{6}A^{7}A^{8}T^{9}G^{10}G)_2^{3'}$ (2b)

We have shown earlier[20] the influence of ammonia, NaCl and pH on the intensity of the water–2HA cross peaks for $d^{5'}(^{1}C^{2}C^{3}\mathbf{A}^{4}\mathbf{T}^{5}\mathbf{T}^{6}\mathbf{A}^{7}\mathbf{A}^{8}\mathbf{T}^{9}G^{10}G)_2^{3'}$ (**2b**). In the present study, the hydration of $d^{5'}(^{1}C^{2}G^{3}\mathbf{A}^{4}\mathbf{T}^{5}\mathbf{T}^{6}\mathbf{A}^{7}\mathbf{A}^{8}\mathbf{T}^{9}C^{10}G)_2^{3'}$ (**1b**) was compared with that of $d^{5'}(^{1}C^{2}C^{3}\mathbf{A}^{4}\mathbf{T}^{5}\mathbf{T}^{6}\mathbf{A}^{7}\mathbf{A}^{8}\mathbf{T}^{9}G^{10}G)_2^{3'}$ (**2b**) under identical experimental conditions (i.e. 4 mM concentration in 0.4 ml of 90% H_2O–10% D_2O with no buffer added) [see Fig. 4(A) and (B) for **1b** and Fig. 4(C) and D for **2b**].

In the NOESY and ROESY spectra of both duplexes **1b** and **2b** at 15 °C [Fig. 4(A)–(D)] and 10 °C (data not shown), three cross peaks are found between bound water and H2A protons ($^{3}\mathbf{A}$, $^{6}\mathbf{A}$, and $^{7}\mathbf{A}$). In the ROESY spectra, all three peaks are very strong with negative sign [Fig. 4(A) and (C)], which, however, showed different signs in the NOESY spectra [Fig. 4(B) and (D)].

In NOESY spectra for duplexes **1b** and **2b**, the water–$H2^{3}A$ cross peak is negative as in the ROESY spectra, indicating that $\sigma_{NOE}/\sigma_{ROE} > 0$. This is especially clear for duplex **1b** in which $H2^{3}A$ does not overlap with any other proton resonances. For duplex **2b** at 10 and 15 °C, the $H2^{3}A$ resonance overlaps with aromatic protons of ^{10}G and ^{9}G residues and partly with the terminal ^{1}C residue, which may potentially show cross peaks with bound water molecules. Nevertheless, the present data [Fig. 4(D)] qualitatively allow us to conclude that at least the water–$H2^{3}A$ cross peak of duplex **2b** is not positive under our present experimental conditions. Indeed, we have earlier found[20] a clear positive water–$H2^{3}A$ cross peak in the NOESY spectra of duplex **2b** *only* in the presence of an ammonia catalyst or at alkaline pH [see Fig. 2(Ai)].[20]

These data for **1b** and **2b** unambiguously indicate that the residence time of the bound water molecule near the $H2^{3}A$ proton under the present experimental conditions is <0.36 ns,[21–23] which is a well known behaviour[17,24,25] for the water located in the major groove of native DNA in the

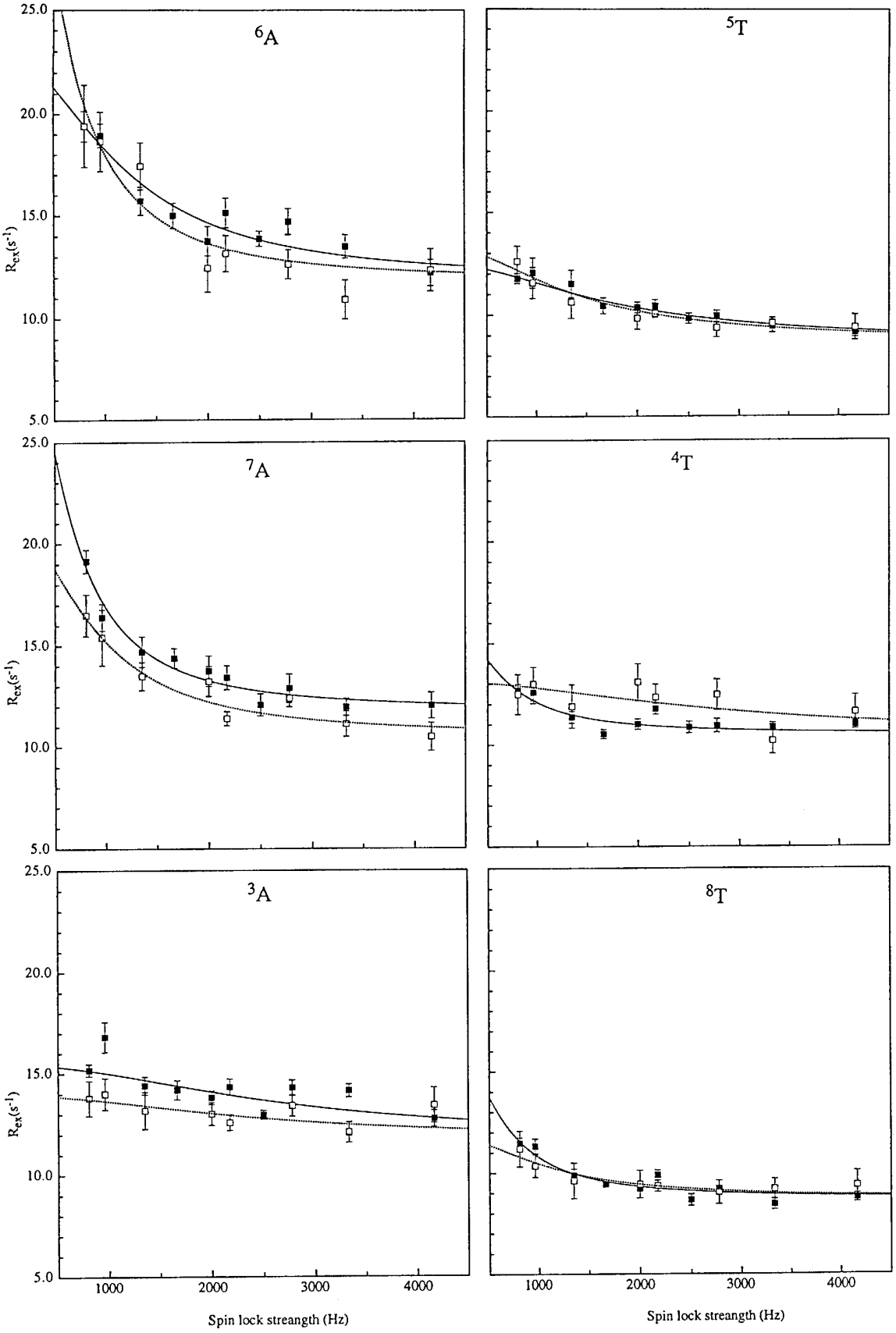

Figure 3. Transverse relaxation rates, $R_{1\rho}$, of $^{13}C(2')$ plotted against effective field strength of spin lock, $\omega_1/2\pi$, for six residues (panels are marked with names of residues) in duplexes $d^{5'}(^1C^2G^3\mathbf{A}^4\mathbf{T}^5\mathbf{T}^6\mathbf{A}^7\mathbf{A}^8\mathbf{T}^9C^{10}G)_2^{3'}$ (**1b**) (□) and $d^{5'}(^1C^2C^3\mathbf{A}^4\mathbf{T}^5\mathbf{T}^6\mathbf{A}^7\mathbf{A}^8\mathbf{T}^9G^{10}G)_2^{3'}$ (**2b**) (■) at 25 °C. Error bars represent the standard deviation of $R_{1\rho}$. The dashed and solid curves for the duplexes **1b** and **2b**, respectively, are the best least-squares fits of Eqn (2) with τ_{ex} and $\Delta\Omega$ as free variables. $1/T_{1\rho}^{\infty} = 11.76\,s^{-1}$ was used for simulation of the curves for A residues, $1/T_{1\rho}^{\infty} = 8.7\,s^{-1}$ for ^8T and ^5T residues and $1/T_{1\rho}^{\infty} = 10.5\,s^{-1}$ for ^4T residue.

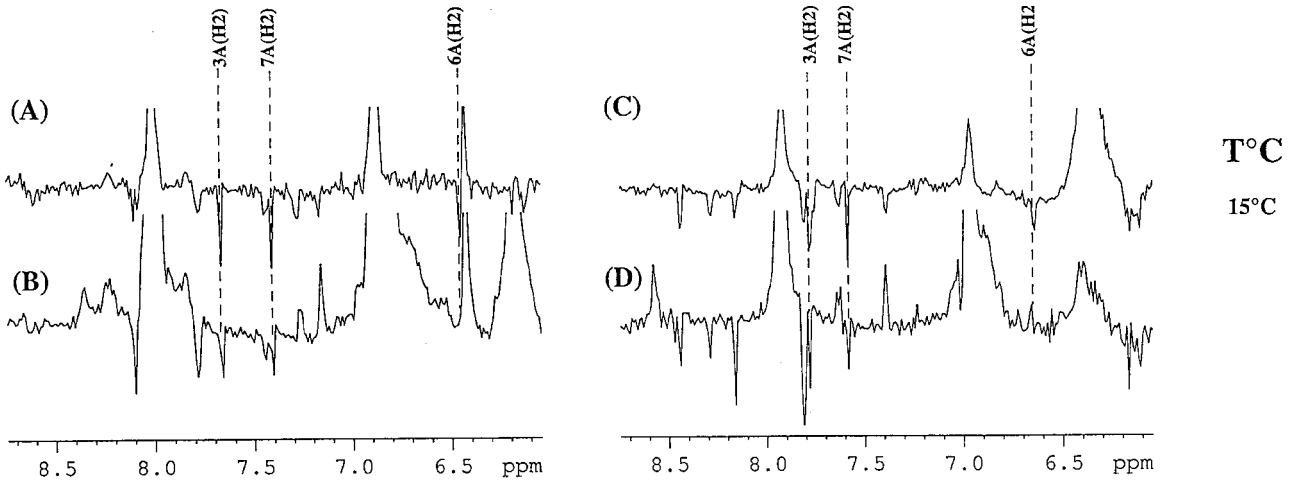

Figure 4. Comparison (at 15 °C) of the cross-section through the NOESY [(B) and (D)] and ROESY [(A) and (C)] spectra of duplex $d^{5'}(^1C^2G^3\mathbf{A}^4\mathbf{T}^5\mathbf{T}^6\mathbf{A}^7\mathbf{A}^8\mathbf{T}^9C^{10}G)_2^{3'}$ (**1b**) [(A) and (B)] and $d^{5'}(^1C^2C^3\mathbf{A}^4\mathbf{T}^5\mathbf{T}^6\mathbf{A}^7\mathbf{A}^8\mathbf{T}^9G^{10}G)_2^{3'}$ (**2b**) [(C) and (D)] between 8.7 and 7.0 ppm. The NOESY and ROESY spectra were recorded at 120 and 60 ms mixing times, respectively. In this field region, 8.7–7.0 ppm, the water–DNA NOE/ROE cross peaks with H2A are shown and the assignments of the DNA protons are given at the top of the panels.

proximity of methyl groups of thymidine moieties (Me-T). Indeed, the cross peaks corresponding to water–(Me-T) are negative for both duplexes **1b** and **2b**[20] (data not shown). It is noteworthy that this result is independent of the concentration of duplex **1b** in the concentration range 2–8 mM.

It is noteworthy that these observations are in complete agreement with those found for duplex **3**, $d^{5'}(^1G^2C^3A^4T^5T^6A^7A^8T^9G^{10}C)_2^{3'}$, where a negative NOE for the water–$H2^3A$ cross peak was detected.[15]

In contrast to the water–$H2^3A$ cross peak in the NOESY spectra of both **1b** and **2b** [Fig. 4(B) and (D)], the water–$H2^6A$ cross peak vanishes to zero or becomes slightly positive. In the absence of an ammonia catalyst, which could catalyse proton exchange and induce the magnetization relay transfer pathway from water to the H2A proton,[20] the positive NOE cross peak indicates that the residence time for the bound water is ≥ 0.36 ns. This is again in full agreement with literature data obtained for duplex 3.[26]

The situation is more complex, however, for the water–$H2^7A$ cross peak. In the NOESY spectra of duplex **1b** it is negative and likely to be less intense than for water–$H2^3A$ (overlap makes the integration impossible). For duplex **2b**, it is varies from a small negative peak to zero depending on the temperature.[20] Unfortunately, for both duplexes **1b** and **2b**, the $H2^7A$ resonance partially overlaps with $H6^1C$ and $H6^2C$ protons, which could contribute to the intensity of water–$H2^7A$ cross peaks. The similar discrepancy in the sign of the water–$H2^7A$ cross peak in duplex **3** and in other heteroduplexes has been noted earlier.[26]

The results of this study in conjunction with those available in the literature[26] allow us to conclude that for sequences with **ATTAAT** tracts which are immediately preceded and followed by a CG base pair, the sign of the water–H2A cross peak seems to be changed from negative for water–$H2^3A$ to positive water–$H2^6A$ in the NOESY spectra. Hence the correlation of the sign of the NOE[21–23] with that of the residence time of the bound water molecule allows us to assume that water–$H2^3A$ contact has a residence time of <0.3 ns, which means that water is weakly bound. On the other hand, the residence times of water–$H2^7A$ (~ 0.3 ns) and water–$H2^6A$

Table 3. Melting points and thermodynamics of duplexes

DNA duplexes	No.	T_m (°C)	ΔH° (kJ mol^{-1})	ΔS° kJ mol^{-1} K^{-1}	$-T\Delta S^\circ$ (kJ mol^{-1})	ΔG° (kJ mol^{-1})
$5'd(^1C^2\mathbf{G}^3A^4T^5T^6A^7A^8T^9\mathbf{C}^{10}G)3'$ $3'd(^{10}G^9\mathbf{C}^8T^7A^6A^5T^4T^3A^2\mathbf{G}^1C)5'$	**1b**	36.7[a]	−212.8	−0.59	176.3	−36.5
$5'd(^1C^2\mathbf{C}^3A^4T^5T^6A^7A^8T^9\mathbf{G}^{10}G)3'$ $3'd(^{10}G^9\mathbf{G}^8T^7A^6A^5T^4T^3A^2\mathbf{C}^1C)5'$	**2b**	32.8[a]	−157.0	−0.42	124.3	−32.7
$5'd(^1\mathbf{G}^2C^3C^4A^5A^6A^7C^8A^9T)3'$ $3'd(^{19}\mathbf{C}^{18}G^{17}G^{16}T^{15}T^{14}T^{13}G^{12}T^{11}A^{10}C)5'$	**6**	37.4[b]	−253.7	−0.72	213.7	−40
$5'd(^1\mathbf{C}^2C^3C^4A^5A^6A^7C^8A^9T)^{3'}$ $3'd(^{19}\mathbf{G}^{18}G^{17}G^{16}T^{15}T^{14}T^{13}G^{12}T^{11}A^{10}C)5'$	**7**	34.3[b]	−250.4	−0.71	212.7	−37.7

[a] At a concentration of total single strand of 20 μM.
[b] At a concentration of total single strand of 6 μM.

(>0.3 ns) suggest that water is slightly more bound at these centres than at H2^{3}A.

Thermodynamic study of the DNA duplexes

We also compared the thermodynamic stabilities of duplexes **1b** and **2b** using UV spectrophotometry at the same buffer composition as used in the NMR study (see Experimental). The T_m values (taken at a 20 μM concentration of a single strand of duplexes), ΔH°, ΔS° and ΔG° for duplexes **1b** and **2b** are presented in Table 3.

Based on these data, the following observations can be made: (1) duplex **1b** is thermodynamically more stable than duplex **2b** (~4° difference in their T_m values); (2) ΔH° and ΔS° for duplex **1b** are higher than for duplex **2b**; (3) the comparison of the enthalpic and entropic contributions to the free-energy of stabilization of these two isomeric duplexes shows (Table 3) that ΔH° for duplex **1b** is well compensated by an increase in ΔS° in counterdistinction with duplex **2b**, thereby explaining the only ~4° higher T_m for the former duplex compared with the latter. It is noteworthy that the number of hydrogen bonds in both duplexes is the same and the substitution of the GC base pair of duplexes **1b** and **2b** by CG changes only the stacking interaction between GC and the third AT base pair and with GC with terminal CG base pairs.

DISCUSSION

A few reports have appeared on the flexibility[27–29] of triplets containing a TG base pair step in DNA duplexes. The structure determination and analysis of the helix parameters in d(C*ATG*GCCATG)$_2$ (**4**) by means of comparative NMR and crystallographic data have shown[29] a specific local conformation of the TG/CA base pair step. Considerable differences between the NMR and x-ray structures of duplex **4** have also been found in the local conformation of the TG/CA base pair step. The solution NMR structure of duplex **4** is characterized by a positive roll angle. Large positive roll angles have also been observed in several DNA duplexes.[30,31] Recently, an empirical correlation between the level of propeller twist and the flexibility of dinucleotide steps was also scrutinized and established.[32]

Direct evidence supporting a conformational exchange process also emerges from the observation of the large amplitude (in the range of 130–250 Hz) and slow motions ($\tau_{ex} = 130$ μs) for the ^{4}A residue (within the C^{4}A step), basing on rotating frame relaxation measurements of $R_{1\rho}$ of ^{13}C(1′) for d(^{1}C^{2}G^3*C*^{4}*A*^{5}A^{6}ATTTGCG)$_2$[27] (**5**). These literature data are consistent with our present observation that the ^{2}C^3**A** step in **2b** indeed provides flexibility of the ^{3}**A** residue. This conclusion is reinforced by the fact that the ^{2}G^3**A** step in duplex **1b** does not provide the similar flexibility for ^{3}**A** as found for the corresponding residue in the ^{2}C^3**A** step in **2b**.

Another conclusion can be drawn from the comparison of our data with those in the literature for d(^{1}C^{2}G^3*C*^{4}*A*^{5}A^{6}ATTTGCG)$_2$[27] (**5**), that the d(−^{6}A^{7}T−) step in its core part shows considerably different mobility to the d(−^{5}T^{6}A−) step in our duplexes **1b** and **2b**. No additional relaxation pathways induced by slow motions have been observed for other residues (^{3}C, ^{6}A, ^{7}T, ^{8}T and ^{9}T)[27,28] in duplex **5**. In our duplexes **1b** and **2b**, however, ^{6}**A** experiences conformational exchange in the microsecond dynamic range with large amplitudes.

Moreover, for all A·T base pairs of duplexes **1b** and **2b**, the **T** residue does not exhibit a slow conformational exchange process with large amplitude on the microsecond time-scale compared with the flexible **A** residue. These observations are in complete agreement with data reported for duplex **5**.[28]

The additional relaxation process in the microsecond range found for the ^{4}A residue of duplex **5**, d(^{1}C^{2}G^3*C*^{4}*A*^{5}A^{6}ATTTGCG)$_2$[27], has been assumed to reflect a special dynamic process of the AAATTT tract, which supports the spine of hydration theory.[27] The large dynamic process of the ^{4}A residue is believed[27] to relate to the gradual increase in the compression of the minor groove by reaching a minimum at the ApT step,[33] supporting the spine of hydration observed in x-ray studies.[34] The latest x-ray study[35] of duplex **5** shows that the hydration motif of this duplex is a ribbon rather than a spine. The NMR study,[36] however, supports the spine for hydration theory[34] in this duplex. Water–H2A NOE contacts were detected at the central AT step and it was found that these data contradict the x-ray results.[35] However, an NMR study of hydration of r(^{1}C^{2}G^3*C*^{4}*A*^{5}A^{6}ATTTGCG)$_2$, which is an analogue of the DNA duplex **5**, unambiguously shows the presence of a long-lived water molecule close to H1′ despite the wide and shallow minor groove of RNA.[37] It was concluded[37] that chemical factors such as hydrogen bonding of water with the hydroxyl groups in RNA is more important for hydration than the minor groove width. This conclusion has been confirmed in our recent work[38] on the antisense DNA duplex containing hydrophilic (6′-α-hydroxy) or hydrophobic (7′-α-methyl) groups in the carbocyclic sugar moiety of thymidines in Dickerson–Drew dodecamer. It has been shown[38] that a change in the residence time of the water molecule takes place in our modified duplex because of the change in the chemical environment with no concomitant change in the width of the minor groove.

In the present study, we attempted to explore whether the dynamics in the microsecond range drives any specific water–DNA interaction by inducing any large conformational transition. This was performed by comparing our NMR-based dynamic and hydration data for duplexes **1b** and **2b** in aqueous solution with those of the hydration data reported using x-ray studies of the corresponding unlabelled duplexes, d$^{5'}$(^{1}C^{2}G^{3}A^{4}T^{5}T^{6}A^{7}A^{8}T^{9}C^{10}G)$_2^{3'}$ (**1a**) and d$^{5'}$(^{1}C^{2}C^{3}A^{4}T^{5}T^{6}A^{7}A^{8}T^{9}G^{10}G)$_2^{3'}$ (**2a**), which share the central ^{3}A^{4}T^{5}T^{6}A^{7}A^{8}T tract with a single base change at the terminus.

According to the x-ray structure analysis,[10] the minor groove is narrow through the middle of the helix for d$^{5'}$(^{1}C^{2}C^{3}A^{4}T^{5}T^{6}A^{7}A^{8}T^{9}G^{10}G)$_2^{3'}$ (**2a**) with a single well-defined spine of hydration. In contrast, the minor groove for d$^{5'}$(^{1}C^{2}G^{3}A^{4}T^{5}T^{6}A^{7}A^{8}T^{9}C^{10}G)$_2^{3'}$ (**1a**) has been found

to be narrow at the ends of the $^{3}A^{4}T^{5}T^{6}A^{7}A^{8}T$ segment but widens at the centre. Nevertheless, the difference in the minor groove width has been suggested[10] to be the result of crystal packing force. In the present NMR study, we found that these duplexes are indeed different, and are distinguished by different mobilities of ^{3}A and ^{6}A. One major difference between the x-ray study of duplexes **1a** and **2a** and our present NMR study of **1b** and **2b** regarding the spine of hydration is that whereas the x-ray study produced different hydration behaviours for these duplexes, we found very similar water–H2A NOE contacts for H2^{3}A and H2^{6}A for both duplexes **1b** and **2b**, which are comparable to those found for duplex **3**[26] with an identical AT tract. This perhaps validates the assumption[10] of the x-ray study that the difference in hydration observed in the solid state is indeed due to the packing forces and not to the changes in the chemical environment. The difference in the microsecond dynamics between these two duplexes, observed in the present work, also does not seem to dictate any different hydration behaviour in solution.

The residence times of the bound water molecules in water–H2^{3}A and water–H2^{7}A contacts are very short (<0.3 ns and ~0.3 ns, respectively), which means that water is weakly bound despite the fact that these residues, ^{3}A and ^{7}A, belong to dynamically more stable base pairs, ^{3}A–^{8}T and ^{4}T–^{7}A. These observations are consistent with recent experimental observations that the residence time of the bound water molecule in the minor groove of DNA duplex is indeed short.[20,42,43]

The thermodynamic data, T_m, ΔH°, ΔS° and ΔG°, for these two duplexes, **1b** and **2b**, are in full agreement with the NMR data, showing that the mobility in duplex **2b** is larger (with a lower melting point and ΔG°) compared with duplex **1b**. It seems that a stacking interaction between the second GC and third AT base pair and with terminal CG base pairs are essentially different in duplexes **1b** and **2b**.

In order to verify the influence of the base-stacking interaction of the terminal base pair on the thermodynamic stability of duplexes, we recently[44] performed a UV study of two hetero oligo-DNA duplexes, $d^{5'}(^{1}G^{2}C^{3}C^{4}A^{5}A^{6}A^{7}C^{8}A^{9}T)^{3'}\cdot d^{5'}(^{10}C^{11}A^{12}T^{13}G^{14}T^{15}T^{16}T^{17}G^{18}G^{19}C)^{3'}$ (**6**) and $d^{5'}(^{1}C^{2}C^{3}C^{4}A^{5}A^{6}A^{7}C^{8}A^{9}T)^{3'}\cdot d^{5'}(^{10}C^{11}A^{12}T^{13}G^{14}T^{15}T^{16}T^{17}G^{18}G^{19}G)^{3'}$ (**7**), in which only terminal residues are switched. As is evident from Table 3, the switch of terminal GC base pairs in duplexes **6** and **7**, compared with the present duplexes **1b** and **2b**, in which the second base pair from the termini is switched, does not lead to any significant difference in the ΔH° and ΔS° contributions to ΔG°. This is most probably due to a strong end-fraying effect of the terminal base pair in **6** and **7** compared with the second GC base-pair swich, as in **1b** and **2b**. This leads us to conclude that the intrastrand second and third base–base stacking interaction, i.e. GA in **1b** and CA in **2b**, has more influence on the overall stability and dynamic behaviour of the duplex than the first and second base-base stacking.

Acknowledgments

The authors thank the Swedish Board for Technical and Engineering Research (TFR), the Swedish Natural Science Research Council (NFR) (contract No. K-KU 12067-300 to A.F. and K-AA/Ku04626-321 to J.C.) and the Wallenbergsstiftelsen for generous financial support.

REFERENCES

1. King GC, Harper JW, Xi Z. *Methods Enzymol.* 1995; **261**: 436.
2. Maltseva TV, Földesi A, Chattopadhyaya J. *Magn. Reson. Chem.* 1998; **36**: 227.
3. (a) Meekhof AE, Freund SMV. *J. Biomol. NMR* 1999; **14**: 13; (b) Orekhov VV, Pervushin KV, Arseniev AS. *Eur. J. Biochem.* 1994; **219**: 887; (c) Szyperski T, Luginbuhl R, Otting G, Guntert P, Wüthrich K. *J. Biomol. NMR* 1993; **3**: 151; (d) Banci L, Bertini I, Cavazza C, Felli IC, Koulougliotis D. *Biochemistry* 1998; **37**: 12320.
4. Palmer AG III. *Curr. Opini. Struct. Biol.* 1997; **7**: 732.
5. Wang Y-S. *Concepts Magn. Reson.* 1992; **4**: 327.
6. (a) Constantine KL, Friedrichs MS, Wittekind M, Jamil H, Chu C-H, Parker RA, Goldfarb V, Mueller L, Farmer BT. *Biochemistry* 1998; **37**: 7965; (b) Munder FAA, de Graff RA, Kaptein R, Boelens R. *J. Magn. Reson.* 1998; **131**: 351.
7. Davis DG, Perlman ME, London RE. *J. Magn. Reson. B* 1994; **104**: 266.
8. Blackledge MJ, Brüschweiler R, Griesinger C, Schmidt JM, Xu P, Ernst RR. *Biochemistry* 1993; **32**: 10960.
9. (a) Mandel A, Akke M, Palmer AG III. *Biochemistry* 1996; **35**: 16009; (b) Akke M, Palmer AG III. *J. Am. Chem. Soc.* 1996; **118**: 911.
10. (a) Quintana JR, Grzeskowiak K, Yanagi K, Dickerson RE. *J. Mol. Biol.* 1992; **225**: 379; (b) Goodsell DS, Kaczor-Grzeskowiak M, Dickerson RE. *J. Mol. Biol.* 1994; **239**: 79.
11. Földesi A, Maltseva TV, Chattopadhyaya J. *Nucleosides Nucleotides* 1999; **18**: 1377.
12. Maltseva TV, Földesi A, Chattopadhyaya J. *Magn. Reson. Chem.* 1999; **37**: 203.
13. (a) Shaka AJ, Barker PB, Freeman R. *J. Magn. Reson.* 1985; **64**: 547; (b) Shaka AJ, Keeler J, Frenkiel T, Freeman R. *J. Magn. Reson.* 1983; **52**: 335.
14. (a) Palmer AG III, Rance M, Wright PE. *J. Am. Chem. Soc.* 1991; **113**: 4371; (b) Nicholson LK, Kay LE, Baldisseri DM, Arango J, Young P, Bax A, Torchia DA. *Biochemistry* 1992; **31**: 5253.
15. Peng JW, Wagner G. *J. Magn. Reson.* 1992; **98**: 308.
16. Peng JW, Thanabal V, Wagner G. *J. Magn. Reson.* 1991; **94**: 82.
17. Maltseva TV, Agback P, Chattopadhyaya J. *Nucleic. Acids. Res.* 1993; **21**: 4246.
18. Otting G, Liepinsh E, Farmer BT II, Wüthrich K. *J. Biomol. NMR* 1991; **1**: 209.
19. (a) Thibaudeau C, Chattopadhyaya J. *Stereoelectronic Effects in Nucleosides and Nucleotides and Their Structural Implications*. Uppsala University Press: Uppsala, 1999; (b) Saenger W. *Principles of Nucleic Acid Structure*. Springer: New York, 1988.
20. Maltseva TV, Roselt P, Chattopadhyaya J. *Nucleosides Nucleotides* 1998; **17**: 1617.
21. Otting G, Liepinsh E, Wüthrich K. *Science* 1991; **254**: 974.
22. Otting G, Liepinsh E, Wüthrich K. *J. Am. Chem. Soc.* 1991; **113**: 4363.
23. Otting G, Wüthrich K. *J. Am. Chem. Soc.* 1989; **111**: 1871.
24. Liepinsh E, Otting G, Wüthrich K. *Nucleic Acids Res.* 1992; **20**: 6549.
25. Kubinec MG, Wemmer DE. *J. Am. Chem. Soc* 1992; **114**: 8739.
26. Jacobson A, Leupin W, Liepinsh E, Otting G. *Nucleic Acids Res.* 1996; **24**: 2911.
27. Gaudin F, Chanteloup L, Thuong NT, Lancelot G. *Magn. Reson. Chem.* 1997; **35**: 561.
28. Gaudin F, Paquet F, Chanteloup L, Beau JM, Thuong NT, Lancelot G. *J. Biomol. NMR* 1995; **5**: 49.
29. Dornberger U, Flemming J, Fritzsche H. *J. Mol. Biol.* 1998; **284**: 1453.
30. Mujeeb A, Kerwin SM, Kenyon GL, James TL. *Biochemistry* 1993; **32**: 13419.
31. Weisz K, Shafer RH, Egan W, James TL. *Biochemistry* 1994; **33**: 354.
32. El Hassan MA, Calladine CR. *J. Biol. Chem.* 1996; **259**: 95.
33. Lipanov AA, Churpina VP. *Nucleic Acids Res.* 1987; **15**: 5833.
34. Drew HR, Dickerson RE. *J. Mol. Biol.* 1981; **151**: 535.

35. Edwards KJ, Brown DG, Spink N, Skelly JV, Neidle S. *J. Mol. Biol.* 1992; **226**: 1161.
36. Fawthrop SA, Yang J-C, Fisher J. *Nucleic Acids Res.* 1993; **21**: 4860.
37. Conte MR, Conn GL, Brown T, Lane AN. *Nucleic Acids Res.* 1996; **24**: 4860.
38. Maltseva TV, Altmann K-H, Egli M, Chattopadhyaya J. *J. Biomol. Struct. Dyn.* 1998; **16**: 569.
39. Geen H, Freeman R. *J. Magn. Reson.* 1991; **93**: 93.
40. Maltseva TV, Földesi A, Chattopadhyaya J. *J. Chem. Soc. Perkin Trans. 2* 1998; 2689.
41. Yamazaki T, Muhandiram R, Kay LE. *J. Am. Chem. Soc.* 1994; **116**: 8266.
42. Denisov VP, Caarlström G, Venu K, Halle B. *J. Mol. Biol.* 1997; **268**: 118.
43. Phan AT, Leroy J-L, Guéron M. *J. Mol. Biol.* 1999; **286**: 505.
44. Ossipov D, Zamaratski E, Chattopadhyaya J. *Nucleosides Nucleotides* 1998; **17**: 1613.

